

The influence of matrix and laser energy on the molecular mass distribution of synthetic polymers obtained by MALDI-TOF-MS

Stephanie J. Wetzel^{a,b,*}, Charles M. Guttman^b, James E. Girard^a

^a Chemistry Department, American University, Washington, DC 20016, USA

^b Polymers Division, National Institute of Standards and Technology, Gaithersburg, MD 20899, USA

Received 8 January 2004; accepted 7 April 2004

Abstract

The molecular mass distribution (MMD) obtained in synthetic polymer characterization by matrix-assisted laser desorption/ionization time-of-flight mass spectrometry (MALDI-TOF-MS) may be biased by preferential desorption/ionization of low mass polymer molecules, preferential ion attachment to larger polymers, or degradation and fragmentation due to the desorption process. In this study we focus on the effect of matrix and laser energy on the MMD of four synthetic polymers of low polydispersity with varying thermal stabilities. The four polymers considered were polystyrene (PS), poly(ethylene glycol) (PEG), poly(methyl methacrylate) (PMMA) and poly(tetrahydrofuran) (PTHF). The matrix in which the polymer is analyzed may also influence the laser energy effect of MALDI and was also considered in this paper. Three common matrixes were considered, dithranol, *all trans*-retinoic acid (RA) and 2,5-dihydroxybenzoic acid (DHB). Statistical analyses of the molecular mass distributions, obtained by varying laser energy and matrixes, reveal trends that can be used to describe the influences of matrix and laser energy on MALDI-TOF-MS data measurement of synthetic polymers. The statistical analysis revealed that the matrix has a greater effect on the polymer MMD than was expected. Polymers analyzed in DHB yielded lower mass moments than polymers analyzed in RA and dithranol. The effects of laser power on the MMD of the polymers were found to be matrix dependent.

© 2004 Elsevier B.V. All rights reserved.

Keywords: Molecular mass distribution; MALDI-TOF-MS; Synthetic polymers

1. Introduction

Matrix-assisted laser desorption/ionization time-of-flight mass spectrometry (MALDI-TOF-MS) has the potential to provide not only molecular mass moment and distribution data for synthetic polymers, but also end group and branching information [1]. But the characterization of synthetic polymers by MALDI-TOF-MS has yielded inconsistent results, indicating that the MALDI-MS determined molecular mass distribution (MMD) is sensitive to instrumental and sample preparation parameters used to obtain the polymer mass spectrum [2–6]. The disparity of these results produces questions about the accuracy and repeatability of the MALDI-TOF-

MS method for characterizing synthetic polymers, therefore, creating a need to define how the MALDI MS instrument parameters effect the molecular mass distribution of the synthetic polymer.

The molecular mass moments of polymers determined by MALDI often differ from those moments determined by other methods of polymer characterization [7,8]. When MALDI-MS spectra are compared with data obtained by size exclusion chromatography (SEC), larger discrepancies are seen for polymers of higher polydispersity [9–14]. When polymers of narrow polydispersities are compared, the SEC and MALDI-MS values tend to have better agreement.

High polydispersity of the polymer is not the only factor that can lead to mass discrimination in MALDI-MS. MALDI-MS analysis of narrow polydisperse polymers can also yield molecular mass moment differences compared to

* Corresponding author. Tel.: +1 412 396 4222; fax: +1 412 396 5683.
E-mail address: wetzels@duq.edu (S.J. Wetzel).

classical methods of polymer characterization, such as NMR and light scattering. In the NIST interlaboratory comparison, the MALDI-MS analysis of polystyrene (PS), polydispersity index of ≈ 1.02 , yielded a lower M_n and M_w than the classical methods [15].

A study by Schriemer and Li [2,3] reported that both instrumentation and sample preparation may influence the MALDI-MS determined MMD. Mass discrimination in MALDI-MS may be attributed to the desorption/ionization process of MALDI, which is not completely understood [16]. Some possible influential parameters of MALDI desorption/ionization method are multimer formation, matrix/analyte ratio, cation concentration, and laser energy [2,3]. The mass discrimination seen in MALDI-MS needs to be examined to gain a better understanding of the MALDI process and its influences on determination of MMD.

One key to understanding the MALDI process and accepting MALDI-MS as a polymer characterization method is to examine whether polymer samples are altered while in the MALDI plume. If the polymer sample is altered in the plume, any influential parameters of this process need to be identified. Also, not all polymers may be influenced in the same way in the MALDI plume. Structure and chain length have a large influence on the physical properties of a polymer. Among properties influenced are thermal stability and propensity to fragment. By considering polymers of varying thermal stability, more can be learned about the effects of the MALDI plume on the polymer MMD.

Four different polymers, polystyrene, poly(ethylene glycol) (PEG), poly(methyl methacrylate) (PMMA), and poly(tetrahydrofuran) (PTHF), were chosen for characterization and analysis by MALDI-TOF-MS. These four polymers were chosen for their varying thermal stabilities. Polystyrene has the highest relative thermal stability, and PTHF has the lowest relative thermal stability [17]. PEG has a higher relative thermal stability than PMMA.

Polystyrene was selected for this study because it is commonly analyzed by MALDI-TOF-MS, is relatively stable and is not expected to fragment in the mass spectrometer. Polystyrene is easily analyzed by MALDI-MS due, in part, to the ease in ionizing polystyrene with silver salts [18]. The PS sample used in this experiment was the same sample that was used in the NIST Interlaboratory Comparison [15].

It is accepted that many polymers degrade in MALDI-TOF-MS resulting in fragment ion peaks in the mass spectrum. PEG and PMMA were chosen for analysis in the current study because each has been shown to fragment in the mass spectrometer [19,20]. The fragmentation in PEG can be identified by the secondary peak series, which can be seen in the low mass region of the polymer mass spectrum. Degradation has also been noted in PMMA [21,22]. A previous experiment showed the effects of laser energy on the molecular mass distribution of PEG and PMMA [19]. In this experiment, a PEG and two PMMA samples were examined by MALDI-MS at two different laser energies. The PEG MMD acquired at the higher laser energy was significantly skewed

toward the lower mass. When PMMA was analyzed at higher laser energies, an effect of laser energy was seen as well [19].

PTHF was chosen for analysis by MALDI-MS because it has very low thermal stability [23]. PTHF has a low ceiling temperature. The ceiling temperature of the polymer indicates the temperature at which the monomer solution must be below in order for polymerization to occur [24]. When PTHF is at a temperature greater than its ceiling temperature, the polymerization reaction can be reversed, and the polymer will depolymerize until only monomer remains. Since PTHF is less thermally stable than the other three polymers, more fragmentation would be expected to occur.

These polymers will be studied by varying the matrix used in the MALDI-MS recipe. Matrix was a parameter considered in the NIST interlaboratory comparison of PS. This study indicated a possible influence of matrix on the low mass tail of the distribution [15]. Matrixes require different laser energies to ablate into the gas phase. Soft matrixes, such as all-*trans*-retinoic acid (RA), require less laser energy than hard matrixes, such as 2,5-dihydroxybenzoic acid (DHB), for desorption in MALDI [25]. The matrixes were chosen to enable study over a wide range of laser energies. The resulting influences of laser energy and matrix on the molecular mass distribution can help to explain the effect of energy (temperature) on the polymer while in the MALDI plume.

PEG, PMMA, PS, and PTHF, were examined at varying laser energies and in various matrixes. The four synthetic polymer samples had narrow polydispersities, ranging from 1.01 to 1.04. Each polymer sample was analyzed in at least two different matrixes. A statistical analysis of the molecular mass distribution was used to reveal effects of the laser energy and the matrix on the MMD. The analysis revealed that matrix type has a greater influence on the polymer MMD than was expected. When polymers were examined in DHB, the moments of the MMD were lower than when examined in RA and dithranol. The effects of laser energy on the MMD of the polymers were found to be matrix dependent. The laser energy had a greater impact on the polymer, usually causing fragmentation, when analyzed in DHB, than for the same polymers examined in RA and dithranol.

2. Experimental

2.1. Samples and reagents

MALDI-TOF-MS analysis was performed on four synthetic polymer samples: (1) a 7000 u polystyrene sample (Polymer Source, Dorval, Québec, Canada), ¹SRM 2888, (2) a 5000 u poly(ethylene glycol) sample (Ameri-

¹ Certain commercial equipment is identified in this article in order to specify adequately the experimental procedure. In no case does such identification imply recommendation or endorsement by the National Institute of Standards and Technology, nor does it imply that the items identified are necessarily the best available for the purpose.

can Polymer Standards Corp., Mentor, OH), 3) a 2900 u poly(tetrahydrofuran) or terathane purchased from Aldrich (Milwaukee, WI) which was fractionated by GPC, and (4) an 8000 u poly(methyl methacrylate) sample (Polymer Standard Services, Mainz, Germany) (see footnote 1). Matrixes used in these experiments were all-*trans*-retinoic acid, dithranol and 2,5-dihydroxybenzoic acid all purchased from Aldrich Chemical and used as received. Salts used in these experiments were sodium trifluoroacetate (NaTFA) and silver trifluoroacetate (AgTFA) purchased from Aldrich and used as received. The solvents used were tetrahydrofuran (THF) stabilized with butylhydroxytoluene (BHT), acetone, chloroform and ethanol (Mallinckrodt Baker, Inc., Phillipsburg, NJ).

2.2. GPC fractionation of PTHF

The PTHF was estimated to have a weight-average molecular mass of 2900 u by Aldrich. The GPC data indicate that this sample has a polydispersity of 1.9. Currently MALDI-TOF-MS techniques only give a good representation of the polymer MMD for polymers of narrow polydispersity, less than 1.2 [13,26]. Therefore, gel permeation chromatography (GPC) was used to fractionate the PTHF.

The chromatography was performed using a GPC 2000 (Waters Corp., Milford, MA). A 0.25% solution by mass of PTHF in THF (stabilized) was fractionated by GPC at 40 °C and at a flow rate of 1 mL/min. The injection volume was 200 μ L. Three columns were used to fractionate the polymer; two were Styragel HT 6E columns and the third was a Styragel HT 2 column (Waters Corp., Milford, MA). The Styragel HT 6E is a mixed bed linear column with an effective PS molecular mass range from 5000 to 10,000,000 u. The Styragel HT 2 is a low molecular mass column with an effective PS molecular mass range of 100 u to 10,000 u. A refractive index detector was used in the determination of the apparent polystyrene molecular moments. The apparent polystyrene molecular masses were calculated using Easi-Cal polystyrene calibrant from Polymer Labs (Amherst, MA) (see footnote 1). The GPC fraction that was used for analysis by MALDI-TOF-MS was determined by GPC to have an apparent PS M_n of 8100 u, an apparent PS M_w of 8400 u and a PD of 1.04.

2.3. MALDI-TOF-MS

The polymer mass spectra were obtained using a Bruker (Billerica, MA) Reflex II MALDI-TOF-MS equipped with dual micro channel plate detectors for both linear and reflectron modes. The acceleration voltage was +25 kV and ions were measured in the reflectron mode. Delayed extraction was optimized for signal-to-noise for the necessary mass range and the medium delay (500 ns) was employed for the collection of all data. A nitrogen laser at 337 nm and a 3 ns pulse width was utilized. The applied laser energy was focused over a spot size of 200 μ m \times 50 μ m. The resolution of the peaks near a molecular mass of 5000 u at FWHM for 100

laser shots was 500. The standard uncertainty of the M_n and M_w obtained by MALDI-TOF-MS is estimated to be 50 and 40 u, respectively. An attenuator was altered to vary the laser energy from 1 to 8 μ J. The laser energy was measured with a LaserProbe Rm-3700 Universal Radiometer (Laser Probe, Inc. Utica, NY) placed after the optics and before the last mirror prior to the source. The laser energy range measured and used for each polymer sample was defined by the ability to obtain measurable mass signal for the polymer. Three MALDI mass spectra were obtained at each laser energy for each polymer sample.

2.4. Sample preparation

PS was analyzed by MALDI-TOF-MS using RA, dithranol, and DHB. The PS samples were solutions of 1:200:1 by mass of PS:Matrix:AgTFA in THF. The resulting solutions of PS in RA and DHB were hand-spotted onto a MALDI probe. The dithranol solution was electrosprayed onto a MALDI probe at 5 kV and 3 μ L/min for 3 min [27]. The dithranol samples were electrosprayed to avoid the large crystalline formations, which occur when dithranol is hand-spotted. These crystalline formations cause poor signal intensity in the MALDI-TOF-MS.

PEG was analyzed using RA, dithranol, and DHB as matrixes. Three 1:25:1 solutions by mass of PEG:Matrix:NaTFA were made for the PEG. The PEG solution in RA was prepared in THF, chloroform was the solvent in the dithranol solution, and the solvent for the PEG in DHB solution was ethanol. The RA and DHB samples were hand-spotted onto a MALDI probe. The dithranol solution was electrosprayed onto the sample probe at 5.0 kV and 5 μ L/min for 2 min.

DHB and RA were the matrixes used in the analysis of PMMA. The PMMA sample solutions were prepared by mixing PMMA, matrix and NaTFA in a 1:100:1 ratio by mass in acetone for RA and THF for DHB. The PMMA solutions were hand-spotted onto the MALDI probe for analysis.

The PTHF sample was analyzed in DHB and RA. For the sample preparation of PTHF in RA 3.6 mg RA was added to 125 μ L of the PTHF GPC fraction. 20 μ L of a 13.3 mg/mL NaTFA/THF solution was then added to the PTHF and RA/THF solution. This solution was then hand-spotted onto the MALDI probe for analysis. The sample solution for the analysis of the PTHF in DHB was prepared by adding 4.6 mg DHB to 125 μ L of the PTHF GPC fraction. Then 40 μ L of a 7.1 mg/mL NaTFA solution was added to the fraction. The final sample was hand-spotted onto the MALDI probe for analysis.

2.5. Sampling method

The MALDI-MS spectra were obtained in a manner to minimize bias due to sample preparation and application. The sample solution, containing matrix, salt and polymer, was applied over the entire probe surface. The samples in dithranol were electrosprayed onto the sample probe, but

all other samples were hand spotted. Generally, the samples were hand-spotted, however, the mass spectra obtained for the polymer samples examined in dithranol with hand spotted sample preparation did not give repeatable M_n values due to a poor signal to noise ratio, so the dithranol samples were electro-sprayed on to the sample probe. The hand spotted sample preparation gave repeatable M_n values for the other matrixes.

Each mass spectrum is the total number of ions from 100 laser shots, as the laser was moved over a site on a stainless steel MALDI target. The laser was in constant motion to prevent possible biases in the molecular mass distribution due to hot spots. The laser was moving constantly regardless of the method of sample application to the MALDI probe.

For the data analysis, three spectra were obtained at each of the laser energies. These three spectra were obtained from three different sites on the 26-site MALDI target. The spectra were obtained from different sites on the MALDI target to reduce the possibility of biases. The laser energy range of the mass spectral data was determined by the sample. Matrix type has a large influence on the laser energy required to obtain a MALDI mass spectrum. For any matrix, the mass spectra were collected at laser energies in which signal was obtained. For any matrix, the data were obtained at randomized laser energy intervals within that range, not in order of increasing or decreasing laser energy.

2.6. Statistical analysis

The M_n of each MMD was calculated and the distribution of the moments was analyzed for outliers. Outliers were defined as moments that fell outside of three standard deviations of the mean M_n of the data. Any outliers were removed from the data sets in subsequent analyses. The polymer mass distributions obtained by MALDI-TOF-MS were also divided by mass into six bins; the first and last bin generally containing a greater mass range, because these bins contain all of the data remaining in the tails of the MMD, the internal four bins containing equal mass ranges. Table 1 lists the mass ranges for the six bins of each polymer examined. The advantage of binning the data is to reveal the effect of laser energy on the tails of the MMD. The number-average molecular mass of each bin was calculated as well as the fraction of the MMD in each bin.

Analysis of variance (ANOVA) was used to determine whether the MMD is influenced by laser energy. The ANOVA of the bin fractions and moments will show which regions of

the MMD are most affected by the laser energy. The significance level of the ANOVA (α) was chosen to be 0.05. ANOVA compares the bin fraction or moment variance at a given laser energy with the bin fraction or moment variance among laser energies to determine if there is a significant influence of laser energy on the bin fraction or moment of the polymer distribution [28]. A bin is said to have a significant variation when the variance among laser energies is greater than the variance of the bin fraction or moment at a given laser energy.

3. Results and discussion

The four polymer samples were analyzed by MALDI-TOF-MS for the influence of matrix type and laser energy on the MMD. Each polymer sample was analyzed in various matrixes while varying the laser energy. The moments and laser energy ranges for the different matrixes for the different polymers are given in Table 2. The values of the moments given in Table 2 are averages of the data taken over all laser energies; therefore, high standard deviations reported in this table are not necessarily a measure of repeatability. Rather high standard deviations of the M_n values given in Table 2 may reflect trends in the data due to effects on the M_n of the laser energy. The M_n of a polymer is often found to vary when different matrixes are used. The M_n of the polymers analyzed in DHB, which requires higher laser energy to ablate the polymer into the gas phase, are all lower than the same polymer samples analyzed in RA, which requires lower laser energy to ablate. This effect is seen to be greatest for the PTHF and the PMMA. This may be a result of the lower thermal stabilities of PTHF and PMMA.

Fig. 1 shows the mass spectra of PS obtained in RA, dithranol, and DHB. The mass spectra of PEG analyzed in RA, dithranol, and DHB are shown in Fig. 2. Fig. 3 shows the mass spectra of PMMA analyzed in RA and DHB. The mass spectra of PTHF in RA and DHB are shown in Fig. 4. In all of these spectra the low mass tails of the spectra in DHB seem to have more signal than the spectra of the equivalent polymer in RA. In Fig. 4, the PTHF mass spectrum in DHB especially shows a larger low mass tail than the spectrum obtained in RA.

In the following paragraphs, the results of the study are given for each polymer separately. The laser energies, at which data was obtained, are given for each polymer. This data is followed by the results of the study of matrix and laser

Table 1
The bin mass ranges for the four polymers

	Bin 1	Bin 2	Bin 3	Bin 4	Bin 5	Bin 6
PS	<4950	4950–5680	5680–6420	6420–7150	7150–7890	>7890
PEG	<3000	3000–3550	3550–4100	4100–4650	4650–5200	>5200
PMMA	<3660	3660–5330	5330–7000	7000–8670	8670–10340	>10340
PTHF	<5000	5000–6250	6250–7500	7500–8750	8750–10000	>10000

These ranges were chosen to best represent the entire molecular mass distribution of each polymer sample.

Table 2

The M_n and M_w and their standard deviations of PS, PEG, PTHF, and PMMA in each matrix in which the polymers were run

Polymer	Matrix	Laser energy (microjoules)	M_n (u)	Standard deviation (u)	M_w (u)	Standard deviation (u)
PS	RA	1.03–2.30	6570	80	6680	70
	Dith	1.34–3.31	6570	30	6670	30
	DHB	3.46–5.52	6260	100	6420	100
PEG	RA	0.96–1.82	4350	60	4410	60
	Dith	1.53–5.03	4080	140	4270	100
	DHB	1.98–7.49	4210	140	4300	100
PMMA	RA	0.88–1.80	7320	70	7610	50
	DHB	3.54–6.88	7000	90	7400	90
PTHF	RA	0.87–2.12	7900	240	8200	240
	DHB	2.32–5.52	6740	170	7140	160

The moments and standard deviations include all data taken over the entire laser energy range.

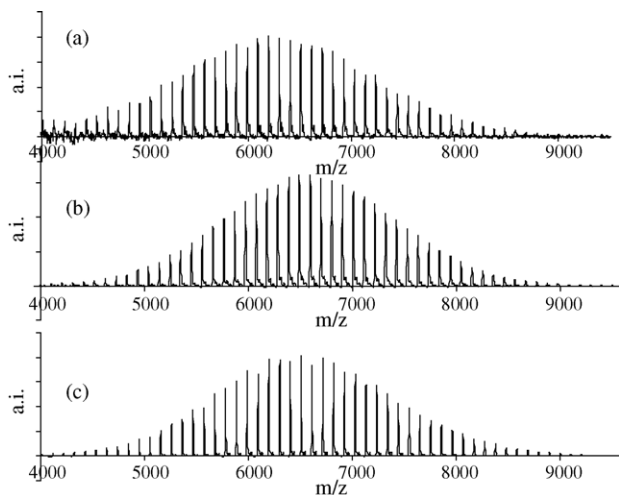


Fig. 1. Mass spectra of PS in (a) DHB, (b) dithranol, and (c) retinoic acid.

energy. The results are given for the analysis of the moments and bin moments of the polymers in the different matrixes and as laser energy changes. The last paragraph of each results section is a discussion of the main effects seen and possible

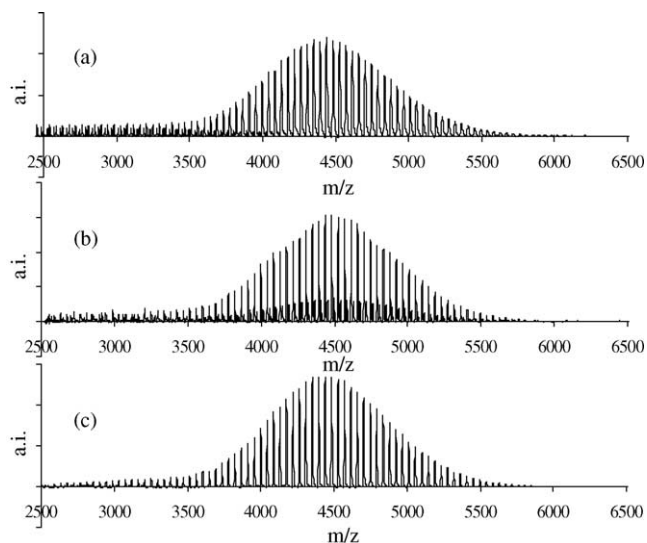


Fig. 2. Mass spectra of PEG in (a) DHB, (b) dithranol, and (c) retinoic acid.

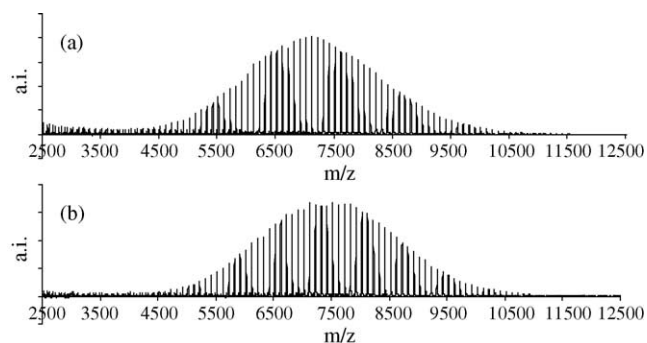


Fig. 3. Mass spectra of PMMA in (a) DHB and (b) retinoic acid.

explanations for these results. The overall effects of matrix and laser power on polymers are discussed in Section 4.

3.1. Polystyrene

Polystyrene was analyzed in three matrixes, dithranol, DHB and RA. Fig. 1 shows the mass spectra of PS taken in these three matrixes. The laser energy varied from 1.25 to 3.25 μJ for PS in dithranol, while the laser energy varied from 1.0 to 2.0 μJ for PS in RA. These matrixes require similar laser energies in order to ablate the polymer sample into the gas phase. Greater laser energies are required when PS

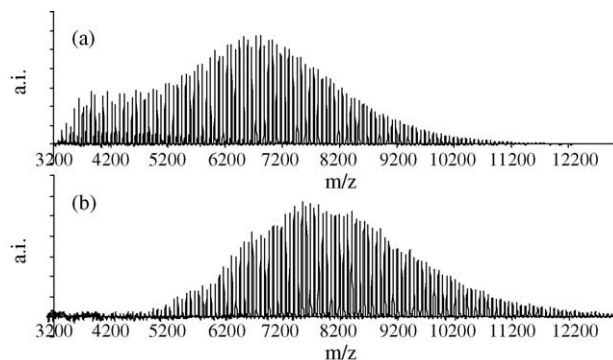


Fig. 4. Mass spectra of PTHF in (a) DHB and (b) retinoic acid.

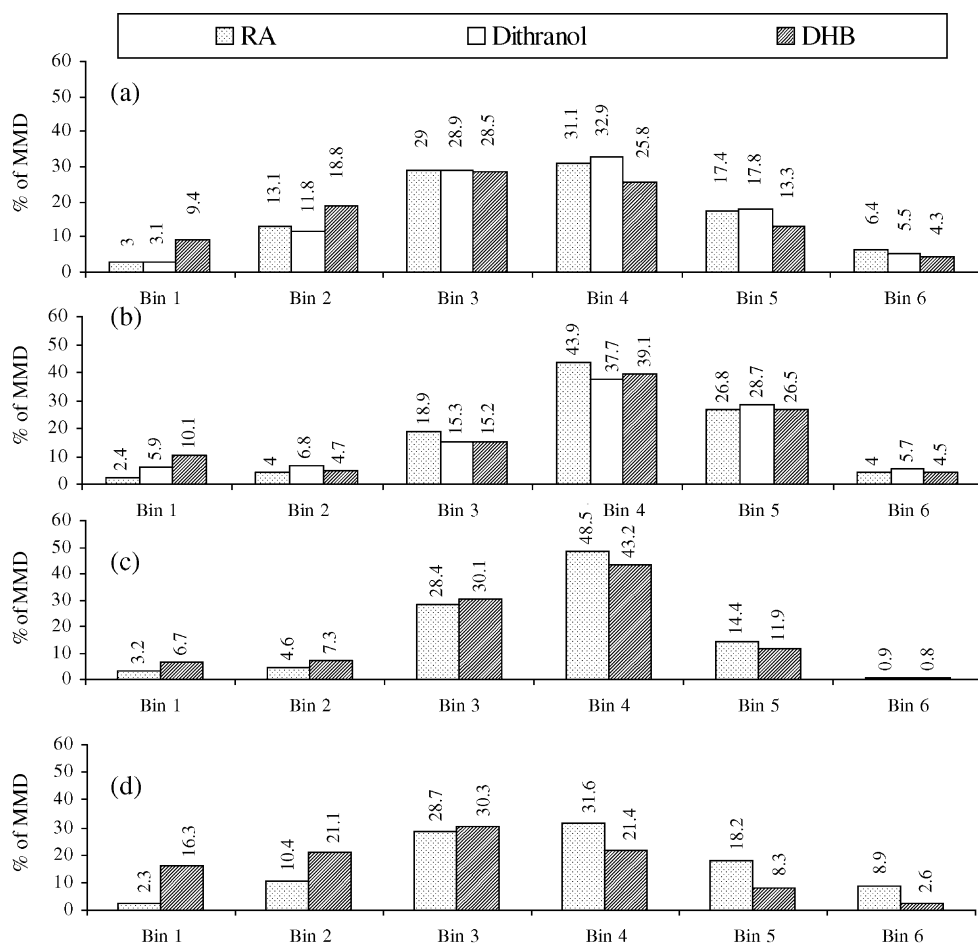


Fig. 5. The histograms represent the distribution of the bins of (a) PS and (b) PEG in RA, dithranol and DHB, and the distributions of the bins of (c) PMMA and (d) PTHF in RA and DHB are shown. The estimated standard uncertainty of the bin percentages obtained by MALDI-TOF-MS is 5%.

is analyzed in DHB. For the analysis of PS in DHB the laser energy was varied from 3.5 to 5.5 μJ .

A histogram of the bins of PS in the three matrixes is shown in Fig. 5a. Bins 1 and 2, the low mass bins of the PS distribution in DHB contain a higher percentage of the MMD than the low mass bins of PS in RA and dithranol. The bins 5 and 6 contain a lower percentage of the MMD in DHB than in RA and dithranol. The data in Table 2 reflect these bin results. The M_n of PS in DHB is 300 u less than those determined for PS in RA and dithranol. The PS analyzed in DHB has greater noise in the low mass tail region than the PS analyzed in RA and dithranol. This noise may bias the moments of the MMD obtained in DHB yielding lower than true values. It should be noted the peak of the MMD in DHB is lower than the peak of the MMD in RA and dithranol.

The number-average molecular masses of polystyrene ranged from 6550 to 6600 u in dithranol, from 6450 to 6650 u in RA and from 6050 to 6550 u in DHB over all laser energies. Although the range of M_n is small for dithranol and retinoic acid, the analysis of variance on the moments of the polystyrene distribution analyzed in these matrixes, shows the variation is influenced by changes in laser energy. With increasing laser energy, the M_n in dithranol shows a maximum,

while the M_n in RA shows a minimum. The PS moments in DHB have a greater variance and are less repeatable, which may explain why the moments of PS in DHB did not show by an ANOVA test any significant variation as laser energy increased.

The six bins mass ranges of the polystyrene molecular mass distribution are given in Table 1. The ANOVA results on the bin moments of PS in RA revealed that the M_n of bins 2, 3 and 5 varied significantly. The mean of bin 2 and 3 decreased as laser energy was increased, the M_n of bin 5 increased as laser energy increased. This indicates that bins 2 and 3 contain more low mass polymer as laser energy increases, and bin 5 contains more high mass polymer as laser energy increases. Of the bin moments of PS in dithranol, bins 2, 3, 4, and 5 were found to have a significant variance. The analysis of the bin moments of PS in dithranol reveals that the M_n of bins 2, 3, 4 and 5 increase as the laser energy is increased. The bins of PS in DHB were not found to have significant variation that may again be due to the increased noise in the data obtained in DHB.

There is an effect of matrix when DHB is the matrix used in the analysis of PS. This effect can be seen in the bin distribution of the MMD (Fig. 5a) and in the M_n (Table 2). A

difference of 300 u in the mean M_n cannot be entirely explained by the amount of noise in the PS mass spectrum. The analysis of the M_n from RA, DHB and dithranol as a function of laser energy does not indicate that the matrix effect is due to laser energy alone. The PS data in DHB shows no trend as laser energy is increased.

3.2. Poly(ethylene glycol)

Polyethylene glycol was analyzed in RA, DHB, and dithranol. The mass spectra of PEG in these matrixes are shown in Fig. 2. The secondary peak series seen in the mass spectrum obtained with dithranol as the matrix is due to PEG molecules ionized by adventitious potassium ions. The laser energy used to obtain the mass spectra of PEG in DHB ranged from 2.0 to 7.5 μJ . The laser energy for the PEG samples analyzed in dithranol ranged between 1.5 and 5.0 μJ . The laser energy ranged from 1.0 to 1.8 μJ for the mass spectra obtained in RA.

The distributions of the mean bins of the MMD of PEG in RA, DHB and dithranol are shown in Fig. 5b. The bin distributions reveal that bin 1 of the PEG distribution analyzed in DHB contains a greater percentage of the MMD than the bins of the MMD analyzed in RA and dithranol. This result indicates that there is greater fragmentation of the PEG occurring when DHB is the matrix. In Fig. 2, a fragmentation peak series can be seen in the low mass tail of the PEG mass spectrum obtained in DHB.

In DHB and in dithranol, the variation in the moments with the laser energies was found to be significant. In DHB the M_n decreases as laser energy is increased, while in dithranol the M_n increases as laser energy is increased. The moments of PEG analyzed in RA were not found to vary significantly by ANOVA. These results are reflected in the moments shown in Table 2. Both DHB and Dithranol have lower mean moments than RA.

The bin analysis of PEG in DHB showed that the M_n of bins 1, 2, 3 and 5 were significantly influenced by laser energy. The M_n in bins 1, 2 and 3 decreased as laser energy increased, the M_n of bin 5 increased as the laser energy was increased. The analysis of the bins of PEG in dithranol revealed that moments of bins 1, 3, 4, 5 and 6 vary significantly. The M_n of bins 1, 3, 4 and 5 increase and the M_n of bin 6 decreases as laser energy increases. The M_n of each bin and the fraction of ions in each bin of PEG in RA were not found to have significant variation as a function of laser energy.

The ANOVA results of the bin data indicate that in DHB the low mass bins increase with increasing laser energy, suggesting that the polymer is fragmenting. The increase of low mass ions can be seen in Fig. 6, in which two PEG mass spectra in DHB are compared, one at low laser energy of 1.85 μJ (Fig. 6a), and the other at a higher laser energy of 5.89 μJ (Fig. 6b). This is also supported by the M_n data found in Table 2. The M_n of PEG in DHB is lower than that of PEG in RA. In dithranol, the high mass bins of PEG increase with increasing laser energy suggesting that more high mass poly-

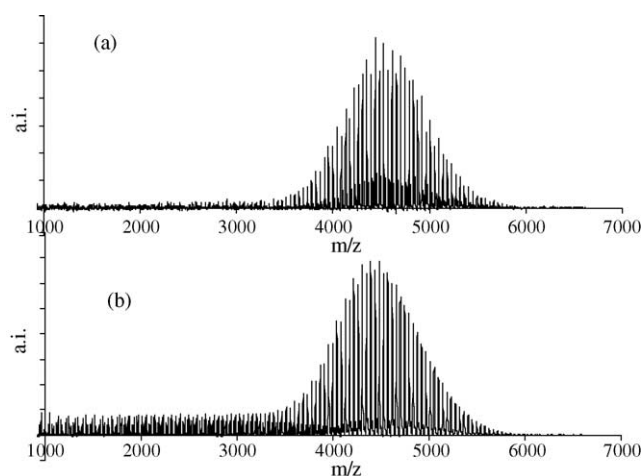


Fig. 6. (a) The mass spectrum of PEG in DHB at a laser energy of 1.85 μJ , (b) the mass spectrum of PEG in DHB at 5.89 μJ .

mer is being ablated into the gas phase as laser energy increases. In RA no effects of laser energy on the MMD of PEG are seen. The PEG samples analyzed in dithranol and RA appear to show few signs of fragmentation in the analysis of the moments and bins. These results indicate that there are effects of laser energy seen for both the PEG analyzed in DHB and dithranol. If the effect of laser energy were independent of the matrix, the expected effect of the laser energy would be the same for each matrix, when the laser energy ranges overlap. However, these results show vastly different effects when PEG was analyzed in DHB and dithranol at the same laser energies. This suggests that an effect of laser energy exists, but it is confounded with a matrix dependent effect.

3.3. Poly(methyl methacrylate)

Fig. 3 shows the mass spectra of PMMA analyzed in RA and DHB. The laser energy was varied from 0.8 to 1.8 μJ when PMMA was analyzed in RA. The PMMA in DHB used laser energies varying from 3.5 to 6.9 μJ . The PMMA in DHB used higher laser energies than those needed for the PMMA in RA to ablate. The lower moments in DHB than RA for PMMA in Table 2 may be influenced by this need for a higher laser energy.

The analysis of PMMA in RA reveals that the M_n does not change significantly with increased laser energy. The mean M_n for PMMA in RA in Table 2 is $(7320 \pm 70 \text{ u})$. The same result is seen when PMMA is analyzed in DHB as laser energy is increased. There is no significant variation of the M_n as laser energy increases. The mean M_n of PMMA in DHB over all laser energies is $(7000 \pm 90 \text{ u})$. The moments of PMMA in DHB are lower than those in RA.

The distributions of the mean bin percentages of PMMA in RA and DHB are shown in Fig. 5c. Bins 1 and 2 of PMMA in DHB contain greater percentages of the MMD than bins 1 and 2 of the MMD obtained in RA indicating more low mass

ions in the DHB MMD than in the RA MMD. The high mass bins of PMMA in DHB contain a lower percentage of the MMD than the high mass bins of PMMA in RA. These results are reflected in the M_n data in Table 2. When the spectra analyzed in DHB and the spectra analyzed in RA are compared, more low mass peaks can be seen in the mass spectra obtained in DHB. Fragmentation of PMMA has been seen before in the MALDI mass spectrometer [29]. This fragmentation is observed as a secondary series seen in the PMMA MMD that is shifted by 32 u less than the main peak series. Thermal degradation studies of PMMA indicate that there is a formation of a radical, and the PMMA chain unzips to monomer [17]. The fragmentation series seen in the mass spectrometer for PMMA is most likely due to the termination of two radical series and this termination results in the loss of a methanol group. The fragmentation series seen in the PMMA spectra explains the bin distribution differences when the polymer is analyzed in the different matrixes.

The ANOVA analysis of the M_n of PMMA for the two matrixes does not show significant variation as laser power is increased. In contrast, the analysis of the bin moments of PMMA in DHB show that bins 3, 4 and 5 vary significantly with laser energy. In fact, in all three bins the moments increase as laser energy is increased. The M_n of the bins of PMMA in retinoic acid were analyzed and were found to increase with increasing laser energy in bins 4 and 5. More high molecular mass polymer is being ablated into the gas phase as laser energy is increased.

The analysis of the PMMA distribution obtained by MALDI-TOF-MS indicates that the matrix used in sample preparation has a significant influence on the polymer mass distribution. The average moments of the PMMA in Table 2 and the bin distributions in Fig. 5c show that the two matrixes yield different results. Fragmentation of PMMA occurs when analyzed in DHB. Fragmentation peaks can be seen in the low mass of the PMMA spectra in DHB in Fig. 3. However, the fragmentation of PMMA does not increase at higher laser energies. Therefore, the fragmentation of PMMA that is observed in the MALDI-TOF-MS is believed due to an effect of the matrix.

3.4. Poly(tetrahydrofuran)

PTHF was analyzed in RA and DHB. The laser energy used for PTHF in RA ranged from 0.8 to 2.1 μJ . The laser energy used for PTHF in DHB ranged from 2.3 to 5.5 μJ . When the PTHF was analyzed in RA no fragmentation series were observed, but in DHB, low mass fragmentation series are present (Fig. 4).

The distribution of the mean bin percentages of PTHF in RA and DHB are shown in Fig. 5d. In RA the first bin contains only 2.3% of the MMD, but in DHB the first bin contains 16.3% of the MMD. Table 2 shows the mean moments of the PTHF mass distribution. The mean M_n of PTHF in DHB is 6740 u and the mean M_n of PTHF in RA is 7900 u. The discrepancies between the mean moments of PTHF analyzed

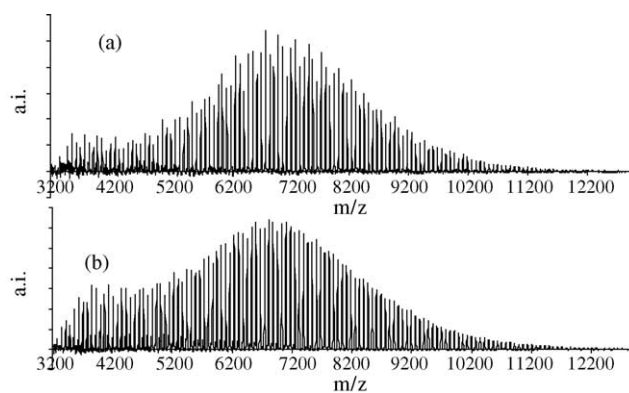


Fig. 7. (a) The mass spectrum of PTHF in DHB at a laser energy of 2.50 μJ and (b) the mass spectrum of PTHF in DHB at 5.10 μJ .

in RA and DHB is greater than those observed for the other polymers examined.

The analysis of the M_n for PTHF in RA revealed that the moments increase with increased laser energy. When PTHF is analyzed with DHB as the matrix, the low mass polymer peaks increase in intensity with increasing laser energy, indicating that the polymer is fragmenting. Fig. 7 shows the mass spectrum of PTHF in DHB at 2.50 (Fig. 7a) and 5.10 μJ (Fig. 7b). In the mass spectrum obtained at a laser energy of 5.10 μJ , more intense fragmentation peaks are observed. The M_n of PTHF in DHB is found to vary significantly with laser energy, but no clear trend exists. The M_n decreases as laser energy increases to $\approx 3.8 \mu\text{J}$ and then increases as laser energy continues to increase.

The bin analysis of PTHF in RA illustrated that the M_n of bins 2, 3, 4 and 5 were influenced significantly as the laser energy is increased. The M_n of these bins increases as laser energy is increased. When DHB was used as a matrix for PTHF, only the moments of bins 1, 3 and 4 were found to vary significantly as laser energy was increased. Bin 1 increased, but bins 3 and 4 decreased for laser energies up to about 4.3 μJ and then began to increase for higher laser energies.

The PTHF MMD shows clear signs of fragmentation, which is expected due to the low thermal stability of the polymer. Fragmentation of the PTHF occurs in DHB, but there is no indication that fragmentation occurs when the PTHF is analyzed in RA. At 2.12 μJ , the M_n of PTHF in RA is 8220 u, and at 2.32 μJ the M_n of PTHF in DHB is 6850 u. The effects of laser energy seen on the PTHF distribution are very different for different matrixes. This indicates again that the effects of laser energy are matrix dependent.

3.5. PEG fragmentation analysis

PEG, unlike the other polymers in this study, fragments in the middle of the chain, producing two fragment ions. The secondary series of peaks seen in the PEG mass spectra is a result of the fragmentation occurring at the oxygen-carbon

bond in the repeat unit of the PEG molecule [20]. Each polymer molecule fragmentation produces two discernible fragment molecules. One PEG fragment molecule will have the same end groups within a single mass unit as the original polymer molecule, and the second fragment ion will have an end group differing by about 16 mass units. If the assumption is made that the PEG molecule is equally likely to fragment on either side of the ether linkage along the polymer chain, then the distribution of the fragmentation peaks with no mass change should be the same as the distribution of the fragment ions with a mass change of 16 mass units due to end group change.

The PEG mass spectra were integrated into peak values using Polymerix (Sierra Analytics, Modesto, CA) (see footnote 1) analysis software. This software has the ability to identify individual peak series and calculate separate distribution information such as moments and polydispersity for the secondary series. Using this software the PEG data were analyzed and then the fragmentation peaks were subtracted

from the mass spectrum. The area of each secondary series fragmentation peak was computed. Since fragmentation may occur on either side of the oxygen, it was assumed that an equal amount of the fragmentation represented by the area of secondary peak would be represented in the main series peak. Thus, the area of each secondary series peak was subtracted from the area of the nearest main series peak. The resulting mass spectra were then analyzed and compared with the original PEG data.

The molecular mass moments of the original data and those calculated after the fragmentation peaks were subtracted from the molecular mass distribution are shown in Table 3 averaged over all laser energies for each matrix. Regardless of matrix, all the moments increase after the fragmentation is subtracted. Changes to the effect of laser energy on the molecular mass distribution due to the subtraction of the fragment peaks are shown in Fig. 8. Each matrix seems to have a different effect on the molecular mass distribution of PEG. When PEG was analyzed in RA, no effect of laser

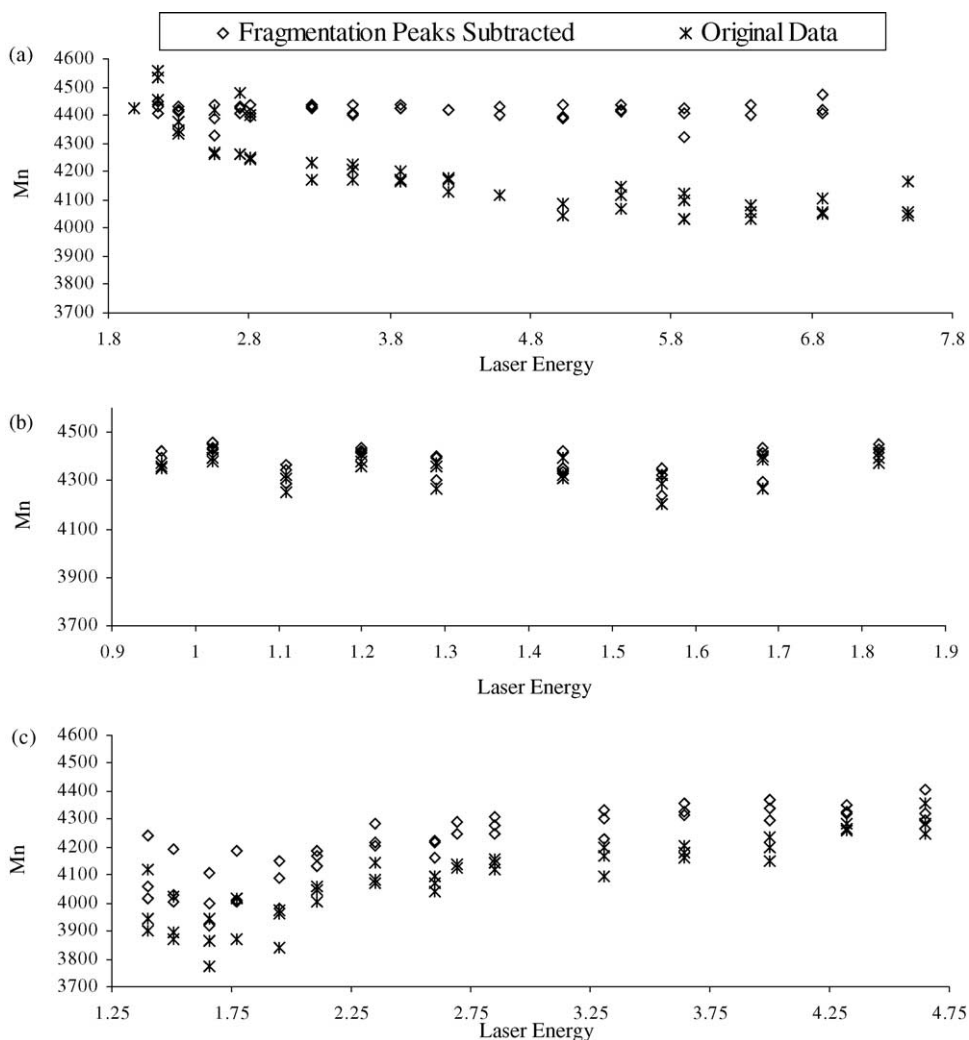


Fig. 8. Plots of the moments of PEG in (a) DHB, (b) RA and (c) dithranol. Both the original data and the moments after the fragmentation peaks were subtracted, as laser energy increases in each matrix.

Table 3

The mean number-average molecular masses and the standard deviation are given for the original PEG mass distributions and for the PEG data with the fragmentation peaks subtracted

Matrix	M_n (u)	S.D. (u)	Corrected M_n (u)	S.D. (u)
RA	4350	60	4390	60
Dithranol	4080	140	4210	130
DHB	4210	140	4420	30

The mean M_n includes data taken at all laser powers.

energy on the molecular mass distribution is seen. The fragmentation and change in the M_n for the PEG in RA is the same for all laser energies. So no change in M_n resulting from the change in laser energy is seen once the influence of fragmentation is removed. The mean M_n of the PEG distributions obtained at the various laser energies increases from $(4350 \pm 60 \text{ u})$ to $(4390 \pm 60 \text{ u})$.

When PEG is analyzed in DHB, the effect of laser energy is different from that in RA after the fragmentation peaks are subtracted. The M_n of PEG in DHB decreased as laser energy increases. However, when the fragmentation peaks are subtracted from the mass distribution, the M_n remains constant, independent of laser energy. Therefore the effect of changing laser energy on the PEG MMD in DHB can be attributed to fragmentation. The mean M_n of the PEG in DHB increased from $(4210 \pm 140 \text{ u})$ without fragmentation subtracted to $(4420 \pm 30 \text{ u})$ with fragmentation subtracted.

The PEG in dithranol has a different result from the other two matrixes. The original data revealed an increase in M_n as laser energy increases. This trend in the data remains after the fragmentation peaks are subtracted from the PEG molecular mass distribution. The M_n of the PEG increases by 200 u at each laser energy after the fragmentation peaks are subtracted. There appears to be a uniform amount of fragmentation at all laser energies. This indicates that although there is an effect of laser energy on the PEG mass distribution, it is not due to fragmentation. This is supported by the mean M_n , which increases from $(4080 \pm 140 \text{ u})$ to $(4206 \pm 130 \text{ u})$. The increase in the M_n that is observed as laser energy increases is due to an increase in the number of high mass molecules getting into the gas phase. The analysis of the bins indicates that a higher number of high mass molecules are present at higher laser energies. Also, when the M_n of the PEG is graphed versus increasing laser energy, the corrected M_n data levels off at an M_n of about 4350 u, approaching a point of equilibrium where all masses of the PEG are getting into the gas phase.

4. Conclusions

The analyses of PS, PMMA, PEG and PTHF reveal that the matrix used in the MALDI sample preparation has an effect on the polymer mass distribution. The data analyses of the four polymers also reveal an influence of laser energy on the molecular mass distribution. But the effect of laser energy is both polymer and matrix dependent. Furthermore, the frag-

mentation of the polymers in the MALDI-MS followed the trends predicted due to the thermal stability of the polymers.

The matrix effects on the polymer MMD can be seen in Table 2 in the M_n and M_w values; the moments of each polymer are lower when analyzed in DHB. A more intense fragmentation pattern is seen in PEG and PTHF when analyzed in DHB. Fragmentation peaks are also seen in PMMA when analyzed in DHB. Little or no fragmentation is seen when these polymers are analyzed with RA or dithranol as the matrix. This effect of matrix is not due entirely to the laser energy required for ablation. The results of the analysis reveal that the matrix plays a greater role in the desorption/ionization process than just the energy needed for the desorption of intact polymer into the gas phase.

Both PEG and PTHF show more fragmentation as laser energy increases when they are analyzed in DHB. The moments of PEG in dithranol increase as laser energy increases, indicating that more high-mass polymer ablates into the gas phase as laser energy increases. An increase in M_n is also seen in PTHF analyzed in RA. The polymer structure, which is already known to influence ionization in MALDI, also influences the effect that the laser energy has on the molecular mass distribution of MALDI-TOF-MS.

Fragmentation was seen in three of the four polymer samples analyzed. Only the PS sample showed no signs of fragmentation. PEG and PMMA show fragmentation peak series when analyzed in DHB. The MMD of PMMA and PEG also had larger low mass tails. Fragmentation is also seen in PTHF in both RA and DHB, and at high laser energies, the entire shape of the MMD changes due to this fragmentation. These results indicate that the thermal stability of a polymer may be a predictor of polymer fragmentation in the MALDI-TOF-MS.

Acknowledgments

S.J.W. thanks the National Science Foundation for the Chemometric Fellowship, Prof. Nancy Flournoy of American University, and NIST for the research capabilities.

References

- [1] U. Bahr, A. Deppe, M. Karas, F. Hillenkamp, *Anal. Chem.* 64 (1992) 2866.
- [2] D.C. Schriemer, L. Li, *Anal. Chem.* 68 (1997) 4176.
- [3] D.C. Schriemer, L. Li, *Anal. Chem.* 68 (1997) 4169.
- [4] C.N. McEwen, C. Jackson, B.S. Larson, *Int. J. Mass Spectrom. Ion Process.* 160 (1997) 387.
- [5] H.C.M. Byrd, C.N. McEwen, *Anal. Chem.* 72 (2000) 4568.
- [6] C. Jackson, B. Larsen, C. McEwen, *Anal. Chem.* 68 (1996) 1303.
- [7] B. Guo, H. Chen, H. Rashidzadeh, X. Liu, *Rapid Commun. Mass Spectrom.* 11 (1997) 781.
- [8] H. Zhu, T. Yalcin, L. Li, *J. Am. Soc. Mass Spectrom.* 9 (1998) 275.
- [9] H. Rashidzadeh, B. Guo, *Anal. Chem.* 70 (1998) 131.
- [10] K. Shimada, M.A. Lusenkova, K. Sato, T. Saito, S. Matsuyama, H. Nakahara, S. Kinugasa, *Rapid Commun. Mass Spectrom.* 15 (2001) 277.

- [11] R.S. Lehrle, D.S. Sarson, *Rapid Commun. Mass Spectrom.* 9 (1995) 91.
- [12] G. Hagelin, J.M. Arukwe, V. Kasparkova, S. Nordbø, A. Rogstad, *Rapid Commun. Mass Spectrom.* 12 (1998) 25.
- [13] G. Montaudo, M.S. Montaudo, C. Puglisi, F. Samperi, *Rapid Commun. Mass Spectrom.* 9 (1995) 453.
- [14] G. Montaudo, D. Garozzo, M.S. Montaudo, C. Puglisi, F. Samperi, *Macromolecules* 28 (1995) 7983.
- [15] C.M. Guttman, S.J. Wetzel, J.E. Girard, W.R. Blair, B.M. Fanconi, R.J. Goldschmidt, W.E. Wallace, D.L. VanderHart, *Anal. Chem.* 773 (2001) 1252.
- [16] R. Knochenmuss, *J. Mass Spectrom.* 37 (2002) 867.
- [17] S.L. Madorsky, *Thermal Degradation of Organic Polymers*, Interscience Publishers, New York, 1964.
- [18] D.C. Schriemer, L. Li, *Anal. Chem.* 68 (1996) 2721.
- [19] J. Axelsson, A. Hoberg, C. Waterson, P. Myatt, G.L. Shiel, J. Varney, D.M. Haddleton, P.J. Derrick, *Rapid Commun. Mass Spectrom.* 11 (1997) 209.
- [20] R.P. Lattimer, *J. Anal. Appl. Pyrolysis* 56 (2000) 61.
- [21] R.S. Lehrle, D.S. Sarson, *Polym. Degrad. Stab.* 51 (1996) 197.
- [22] B.S. Larson, W.J. Simonsick Jr., C.N. McEwen, *J. Am. Soc. Mass Spectrom.* 7 (1996) 287.
- [23] R.P. Lattimer, *J. Anal. Appl. Pyrolysis* 57 (2001) 57.
- [24] H. Elias, R.A. Pethrick (Eds.), *Polymer Yearbook*, 1st ed., Harwood Academic Publishers, New York, 1983.
- [25] B. Thomson, A. Suddaby, G. Lajoie, *Eur. Polym. J.* 32 (1996) 239.
- [26] D. Garozzo, G. Impallomeni, E. Spina, L. Sturiale, F. Zanetti, *Rapid Commun. Mass Spectrom.* 9 (1995) 937.
- [27] R.R. Hensel, R.C. King, K.G. Owens, *Rapid Commun. Mass Spectrom.* 11 (1997) 1785.
- [28] J. Devore, R. Peck, *Statistics: The Exploration and Analysis of Data*, Wadsworth Publishing Co., Belmont, California, 1997.
- [29] K. Martin, J. Spickermann, H.J. Rader, K. Mullen, *Rapid Commun. Mass Spectrom.* 10 (1996) 1471.